

Surface plasmon polariton mediated energy transfer in organic photovoltaic devices

T. D. Heidel, J. K. Mapel, and M. Singh

Department of Electrical Engineering and Computer Science, Massachusetts Institute of Technology, Cambridge, Massachusetts 02139

K. Celebi

Department of Physics, Massachusetts Institute of Technology, Cambridge, Massachusetts 02139

M. A. Baldo^{a)}

Department of Electrical Engineering and Computer Science, Massachusetts Institute of Technology, Cambridge, Massachusetts 02139

(Received 8 June 2007; accepted 29 July 2007; published online 28 August 2007)

The performance of a phthalocyanine-based photovoltaic is boosted in the absorption gap between the phthalocyanine Q and Soret bands. Light absorption is decoupled from exciton diffusion using a light absorbing “antenna” layer external to the conventional charge generating layers. Radiation absorbed by the antenna is transferred into the charge generating layers via surface plasmon polaritons in an interfacial thin silver contact. The peak efficiency of energy transfer is measured to be at least $(51 \pm 10)\%$. © 2007 American Institute of Physics. [DOI: 10.1063/1.2772173]

With a theoretical efficiency similar to conventional inorganic photovoltaics (PVs) and the potential to be manufactured inexpensively,¹ organic semiconductor technology offers a promising route to ubiquitous solar energy generation.¹ Unfortunately, electronic localization in organic semiconductors yields structured optical absorption spectra with pronounced regions of weak absorption. This limits efficiency because the short exciton diffusion length within organic semiconductors demands uniformly strong absorption.²

In this work, we enhance the optical absorption of organic PVs by fabricating a light-absorbing antenna on top of a conventional copper phthalocyanine (CuPC)-based PV (see the device structures in Fig. 1). Light absorbed in the antenna is coupled to the PV using energy transfer via surface plasmon polaritons (SPPs) and radiation into waveguide modes.³ SPPs are a particularly effective energy transfer mechanism as they propagate in the plane of the PV rather than parallel to the incident radiation, thereby providing a more efficient means of pumping thin charge generating structures.⁴ In addition, the SPP mode extends deeply into both dielectric layers, extending the range of energy transfer up to ~ 100 nm. While this distance is much longer than the range of intermolecular Förster energy transfer, the ~ 100 nm energy transfer limit demands antenna materials with absorption coefficients of at least $\alpha = 10^5$ cm⁻¹ to capture sufficient light within the antenna.

Efficient SPP-mediated energy transfer also requires highly efficient photoluminescent (PL) antenna materials. Unfortunately, the PL efficiency η_{PL} of highly absorptive organic semiconductors is typically diminished by intermolecular energy transfer known as concentration quenching. To exploit less absorptive materials with higher η_{PL} , we enclose the antenna within a resonant cavity. As shown in Fig. 1(a), the resonant antenna is employed in place of the silver mirror on the back of the cell. Off-resonance the antenna acts as a mirror, but near the resonant wavelength the antenna

absorption is significantly enhanced, and energy is fed back into the PV cell via SPP-mediated energy transfer. Thus, the resonant antenna structure supplements the performance of the PV cell at resonance, with no degradation off-resonance.

We couple resonant antennas to phthalocyanine-based PV cells, which exhibit a gap in their absorption spectra between the Q and Soret bands. To help fill this gap, we use rubrene, a common organic light emitting device material, which has an absorption coefficient of α

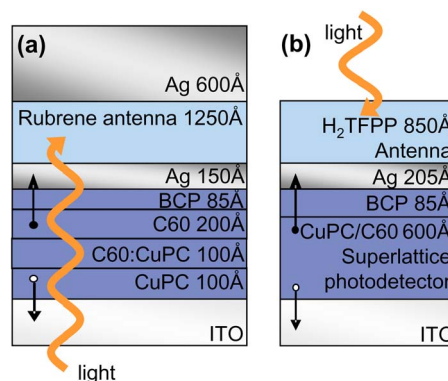


FIG. 1. (Color online) (a) Devices with resonant antenna cavities have the structure glass/indium tin oxide (ITO) (1100 Å)/copper phthalocyanine (CuPC) (100 Å)/CuPC:fullerene (C60) (1:1) (100 Å)/C60 (200 Å)/bathocuproine (BCP) (85 Å)/Ag (150 Å)/30% rubrene in CBP antenna (1250 Å)/Ag (600 Å). To quench or enhance the PL efficiency of the rubrene antenna, we introduce either CuPC or DCJTb, respectively, at 2% weight ratio. Concentration quenching is minimized in the antenna by diluting rubrene with CBP. The devices are illuminated from the glass side. Organic materials were purified by vacuum thermal sublimation prior to use. All materials were deposited by thermal evaporation at $\sim 10^{-6}$ Torr. All active device areas are 0.01 cm². (b) For measurement of energy transfer efficiency, high internal quantum efficiency superlattice photodetectors are used with the structure glass/ITO (1100 Å)/20 alternating layers of CuPC and 3,4,9,10-perylene-tetracarboxylic bisbenzimidazole (PTCBI) (each layer with 15 Å)/BCP (85 Å)/Ag (205 Å)/5, 10, 15, 20-tetrakis(pentafluorophenyl)porphyrin (H₂TFPP) (850 Å). The photoluminescent (PL) efficiency of the H₂TFPP antenna is tuned by adding 4,4'-bis(*N*-carbazolyl)-1,1'-biphenyl (CBP) at varying concentrations. The devices are illuminated from the antenna side.

^{a)}Electronic mail: baldo@mit.edu

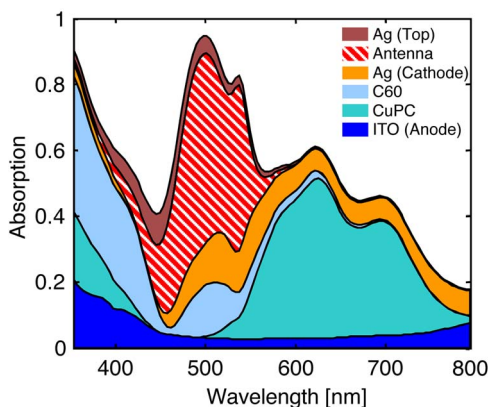


FIG. 2. (Color online) Calculated absorption within the resonant cavity device given illumination from glass side. The tuned cavity results in significantly increased absorption in the antenna layer.

$\sim 10^4 \text{ cm}^{-1}$ at $\lambda \sim 550 \text{ nm}$. Using rubrene as a Förster energy transfer donor for the laser dye 4-(dicyanomethylene)-2-*t*-butyl-6-(1,1,7,7-tetramethyljulolidyl-9-enyl)4H-pyran (DCJTB), $\eta_{\text{PL}} = (90 \pm 10)\%$.

To tune the resonant antenna PV shown in Fig. 1(a), we calculate the expected optical absorption in each layer.² A 1250 Å thick film of 30% rubrene and 2% DCJTB in transparent carbazole biphenyl (CBP) tunes the cavity close to the $\lambda \sim 500 \text{ nm}$ absorption peak of rubrene (see Fig. 2). We model energy transfer within a multilayer organic PV stack by evaluating the Poynting vector \mathbf{P} using dyadic Green's functions.⁵ The wave vector dependence of energy transfer from the antenna to the PV is shown in Fig. 3(a). The energy transfer is plotted against the component of the wave vector parallel to each interface normalized by the wave vector magnitude in the antenna u . Normalized wave vectors with $u < 1$ correspond to radiative modes while those with $u > 1$ correspond to nonradiative energy transfer. For these calculations, the dipole is located in the middle of the antenna layer. Energy transfer occurs predominantly via nonradiative coupling, mediated by SPP modes with $u > 1$. Loss in the silver layers is significant but is minimized by reducing the thickness of the silver cathode. We also model the dipole coupling efficiency to each layer in the PV stack as a function of the dipole distance from the antenna/cathode interface

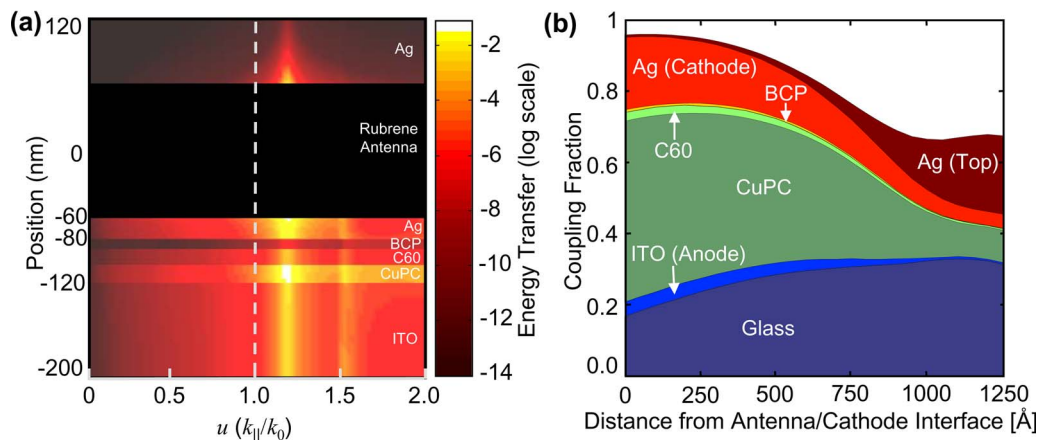


FIG. 3. (Color online) (a) Normalized in-plane wave vector (u) dependence of energy transfer throughout the resonant cavity devices is shown for dipoles oriented perpendicular to the antenna/cathode interface. The parallel geometry is similar. We assume $\eta_{\text{PL}} = 90\%$ at $\lambda = 650 \text{ nm}$. Coupling is greatest for dipoles into modes with $u > 1$, corresponding to surface plasmon polaritons (SPPs). (b) The modeled dipole coupling fraction to each layer in the photovoltaic stack as a function of the dipole distance from the antenna/cathode interface. Coupling to the CuPC and C60 layers results in photocurrent.

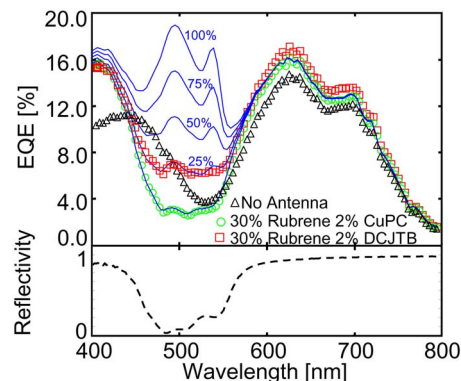


FIG. 4. (Color online) External quantum efficiency (EQE) for resonant antenna devices. Devices with functional external rubrene-based antenna layers exhibit an increase in EQE over the wavelength range where rubrene absorption occurs and the cavity reflectivity decreases. Functional antennas (\square) employ the laser dye DCJTB whereas nonfunctional antennas (\circ) employ the quencher CuPC. The functional antenna shows a significant performance enhancement vs both the quenched antenna and devices fabricated without any antenna (Δ). Comparison with modeling (—) indicates that the energy transfer efficiency is approximately 25%. We also show the expected EQE for energy transfer efficiencies of 0%, 50%, and 75%.

[see Fig. 3(b)]. Near the cathode, $\eta_{\text{ET}} = 54\%$, but the efficiency decreases beyond $\sim 85 \text{ nm}$. Averaged over the antenna, $\eta_{\text{ET}} = 31\%$.

To demonstrate the potential improvement possible using an external resonant antenna in conventional C60/CuPC PV cells, we compare the rubrene/DCJTB antenna device to a control device without the antenna. Quenched antennas were also fabricated with the addition of 2% of the quenching material CuPC instead of DCJTB. External quantum efficiency measurements were made using a xenon lamp with monochromator, chopped at $f = 90 \text{ Hz}$, and measured using a lock-in amplifier. Light intensity was measured with a calibrated silicon photodiode. The external quantum efficiencies of these devices as a function of wavelength are shown in Fig. 4 and compared to the reflectivity of the antenna cavity. The absorption of the antenna (from Fig. 2) and the internal quantum efficiency at the PL maximum of DCJTB, $\eta_{\text{IQE}} = (30 \pm 10)\%$ at $\lambda = 640 \text{ nm}$, are used to determine η_{ET} . This yields $\eta_{\text{ET}} = (25 \pm 10)\%$, consistent with the calculated result of $\eta_{\text{ET}} = 31\%$ in Fig. 3(b). As illustrated, with improved en-

ergy transfer, the efficiency in the spectral gap between absorption peaks could be significantly improved. The absorption modeling also demonstrates that the improved quantum efficiency outside the region where the resonant cavity absorbs is due to reflectivity changes that modify the electric field profile within the device.

While the introduction of the antenna necessarily adds a step into the energy transduction process, it can be employed in spectral regions where the absorption fraction of the PV cell drops below η_{ET} . To reduce the uncertainties in the measurement of η_{ET} , we fabricate an organic superlattice photodetector and antenna without the resonant cavity [see Fig. 1(b)]. This structure should also enhance η_{ET} , since it allows thicker CuPC layers while maintaining a high η_{IQE} , thereby increasing the absorption of SPPs in the charge generating layers.

Under an applied bias, the organic superlattice photodetector is expected to exhibit an internal quantum efficiency close to 100% for excitation by SPP modes.^{4,6} We assume $\eta_{IQE}=100\%$ which gives a lower bound for η_{ET} . The antenna material in this device is tetrakis(pentafluorophenyl)porphyrin (H_2TFPP). It is chosen for its combination of moderate PL efficiency ($\eta_{PL}=2\%–3\%$) and high absorption coefficient ($\alpha=10^6\text{ cm}^{-1}$ at $\lambda=400\text{ nm}$) that allows nearly 100% of incident radiation to be absorbed in the absence of a cavity within the $\sim 100\text{ nm}$ range of SPP-mediated energy transfer.

External quantum efficiency measurements were made at a reverse bias of 3.5 V. The *measured* absorption and PL efficiency of the H_2TFPP antenna is used to determine η_{ET} from the increase in external quantum efficiency $\Delta\eta_{EQE}$, i.e., $\eta_{ET}=\Delta\eta_{EQE}/\eta_{ABS}/\eta_{PL}$. Four H_2TFPP antennas were fabricated with varying PL efficiencies by blending H_2TFPP with different concentrations of CBP. The addition of CBP reduces concentration quenching. To eliminate energy transfer altogether, additional devices were fabricated with nonfunctional antennas comprised of H_2TFPP codeposited with 3.5% of CuPC. Using the quenched antenna as the base line and noting that the absorption of H_2TFPP is $\eta_{abs}=75\%$ for $\lambda\leq 450\text{ nm}$, we obtain $\eta_{ET}=(51\pm 10)\%$, substantially higher than the resonant antenna result (see the inset of Fig. 5). Note that the overall change in quantum efficiency is lower, however, due to the weak η_{PL} of H_2TFPP .

The peak efficiency of SPP-mediated energy transfer in previous studies³ was approximately $\eta_{ET}=5\%$,⁵ too small for

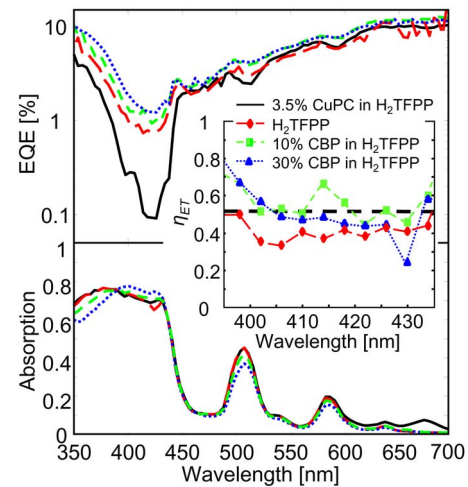


FIG. 5. (Color online) Measurement of energy transfer efficiency using superlattice photodetectors. Top: measurement of external quantum efficiency of devices with different antenna compositions: 3.5% CuPC in H_2TFPP $\eta_{PL}=0\%$ (solid), 100% H_2TFPP $\eta_{PL}=(2.4\pm 0.2)\%$ (long dashed), 90:10 H_2TFPP :CBP $\eta_{PL}=(2.5\pm 0.3)\%$ (short dashed), 70:30 H_2TFPP :CBP $\eta_{PL}=(3.4\pm 0.3)\%$ (dotted). Bottom: absorption spectra of different antenna layers on glass. Inset: calculation of energy transfer efficiency normalized by the PL efficiencies of the various antenna yields $\eta_{ET}=(51\pm 10)\%$.

most applications. The approximately order of magnitude improvement in this work is due to reductions in the thickness of the interfacial silver layer and increasing SPP absorption in the organic semiconductors, which must compete with SPP loss in the silver layer. It is possible to increase the quantum efficiency of an antenna further by optimizing the orientation and position of luminescent antenna excitons with respect to the thin Ag cathode.

This research is supported by DARPA (Grant No. F49620-02-1-0399) and NSF NIRT.

¹S. R. Forrest, MRS Bull. **30**, 28 (2005).

²P. Peumans, A. Yakimov, and S. R. Forrest, J. Appl. Phys. **93**, 3693 (2003).

³P. Andrew and W. L. Barnes, Science **306**, 1002 (2004).

⁴J. K. Mapel, K. Celebi, M. Singh, and M. A. Baldo, Appl. Phys. Lett. **90**, 121102 (2007).

⁵K. Celebi, T. D. Heidel, and M. A. Baldo, Opt. Express **15**, 1762 (2007).

⁶P. Peumans, V. Bulovic, and S. R. Forrest, Appl. Phys. Lett. **76**, 3855 (2000).